Open Access Article

The Ultimate Capacity of Post-Tensioned Segmental Box Girder Bridges with Different Lengths of Segments: An Experimental Study

Alan S. Habib, Omar Q. Aziz

Civil Engineering Department, University of Salahaddin-Erbil, Kurdistan Region, Iraq

Abstract: The flexural behavior of precast concrete segmental box girder is significantly depends on the length of segments. This study aims to investigate the effect of segment length at different compressive strengths of concrete on box girder bridges. In this study, six beams divided into two groups with internal tendons having a constant span of 2400 mm and a different number of segments in each beam for each group were tested to failure to assess the flexural behavior of such bridges when subjected to pure bending under two-point loading. The samples were constructed using High-Performance Concrete (HPC), having a compressive strength of 43.3 and 78.6 MPa for groups 1 and 2, ten shear keys for each segment, four post-tensioning tendons, and a geometry closely resembling the keyed joints of actual segments. Each segmental beam was formed with a different number of segments and different span to depth ratios (L/D). Deflections at mid-span, first crack, concrete surface strains at specified locations, and ultimate load values were recorded during the test. All samples failed due to excessive force in tendons and close to the face of the joints at mid-span. Also, it was observed that segmental beams consisting of three segments with a span to depth ratio = 2.13 recorded greater ultimate load capacity than the other beams with two segments and four segments with = 3.2 and 1.6 in both groups. As for deflection at mid-span, in group1 for the beam with three segments, it was 2.13; the deflection was greater by 13 and 10.6 % than the beams with four and two segments, respectively. For group 2, deflection in the beam with three segments was greater by 4.9% and 19.4% than the beams with two and four segments, respectively.

Keywords: box girder bridge, flexural capacity, high-performance concrete, precast concrete girder bridge, segmental bridge.

不同節段長度的後張拉節段箱樑橋極限承載力試驗研究

摘要：預製混凝土節段箱樑的抗彎性能很大程度上取決於節段的長度。本研究旨在研究不同抗壓強度下的節段長度對箱樑橋的影響。在這項研究中，將六根梁分為兩組，其內部肌腱具有 2400 毫米的恆定跨度，並且每組每根梁中的節段數量不同，進行了測試，以無法評估此類橋樑在承受純彎曲時的彎曲行為。兩點加載。樣品使用高性能混凝土建造，第 1 組和第 2 組的抗壓強度分別為 43.3 和 78.6 兆帕，每個節段有 10 個剪切鍵，4 個後張拉筋，幾何形狀與實際段。每個分段梁由不同數量的分段和不同的跨度與深度比形成。在測試過程中記錄了跨中撓度、第一次裂縫、指定位置的混凝土表面應變和極限載荷值。所有樣品均因肌腱受力過大以及跨中靠近關節面而失敗。此外，據觀察，由跨度與深度比 = 2.13 的三段組成的分段梁記錄的極限承載能力比兩組中的其他兩段和四段梁（分別為 3.2 和 1.6）更大。跨中撓度，三節梁組 1 為 2.13；撓度分別比四段和兩段梁大 13% 和 10.6%。對於第 2 組，三段樑的撓度分別比兩段和四段梁大 4.9% 和 19.4%。

关键词：箱形樑橋、抗彎承載力、高性能混凝土、預製混凝土樑橋、節段橋。

Received: August 12, 2021 / Revised: October 10, 2021 / Accepted: November 11, 2021 / Published: December 30, 2021

About the authors: Alan S. Habib, Omar Q. Aziz, Civil Engineering Department, University of Salahaddin-Erbil, Kurdistan Region, Iraq

1. Introduction

Bridge construction in the form of precast concrete segmental bridges (PCSB) is widely used to construct mid to long-span bridges. It is recognized as a solution to many problems that bridges encounter due to their construction's technique facilities, better durability, practical and rapid assembly, excellent serviceability, competency, low life cycle costs, and aesthetically pleasing [3]. Many detailed kinds of research have been carried out on PCSB in the past decades to understand better the behavior of PCSB, with most of them being done on joints, including dry and epoxy-glued with different geometries [2, 3, and 12]. A comparison in structural behavior between theoretical calculations and experimental work has been described and presented by Tito et al. [10]. A detailed study has been carried out by Wrayosh and Hashim [11] investigating the flexural Behavior of Box Segmental Beams with Internal Tendons Subjected to Repeated and Static Loads. Huang and Hu [9] studied the evaluation of Hathaway precast concrete segmental box girder bridge cracks and concluded that local stresses mainly caused the observed cracks due to the post-tension bars and tendons. Chai et al. [8] investigated the flexural tests and numerical simulation of PCS box-girders with dry joints. The behavior of Precast Prestressed Concrete Segmental Beams (SPPRC) has been investigated by Sherrawi et al. [4]. They have concluded that the behavior of the (SPPRC) is hugely dependent on the behavior of the joints that connects the segments. In this study, an experimental investigation has been carried out to understand better the flexural behavior of segmental post-tensioned beams. Yuan et al. [12, 13] stated that the external tendon stresses and the width of joint openings, the two main causes of the non-linear behavior of segmental prestressed beams, were increased by the different tendon ratios and different types of loads. Experiments were carried out on scaled segmental box girder beams having detailed and geometry similar to the keyed joint of the genuine segmental bridge that has hardly been studied in the literature. Three different concrete strengths, normal strength and two high strengths were used. This study also includes insights into the failure modes, initiation of cracks, load-displacement curves, and failure loads.

2. Experimental Program

2.1. Specimen's Shape, Size, and Dimensions

In this study, nine beams of precast concrete segmental box girder were constructed using a post-tension technique having a total length of 2400 mm. Segments were modeled using a standard section of (3000-1) from AASHTO-PCI-ABSI [1], having a scale factor of 1/8. For practical applicability, the thickness of the webs and the slabs were increased to 120 mm and 100 mm, respectively. The rest of the dimensions and inclination angles were left to be the same as the standard section. The joint interlocking (Fig. 1) was provided by ten shear keys distributed along with the top slab, bottom slab, and height of the webs for fitting the segments and transferring the shear stresses at the time of loading. Table 1 shows complete details of each specimen.

Fig. 1 Location & number of shear keys

2.2. Details of Reinforcement and Prestressing

Deformed steel bars G420-Ø10 mm were used to reinforce the webs, and the slabs had mechanical properties of 543.7 MPa for yield strength and 654.1 MPa for ultimate strength under ASTM-A615 [5]. Fig. 2 and 3 show the reinforcement details of the segments. All the segments were designed to fail in flexural mode; therefore, extra caution against other failure modes was undertaken. For post-tensioning, G1860-Ø12.7 mm with low relaxation was used, according to ASTM-A416 [6].

Four PVC ducts with a 25mm diameter were used to post-tension the segments, as shown in Fig. 4. The jacking force for each strand was 137 kN, and the force transformation to the concrete was done through four steel plates with dimensions of 100x100x8 mm.

Fig. 2 Deformed reinforcement bars

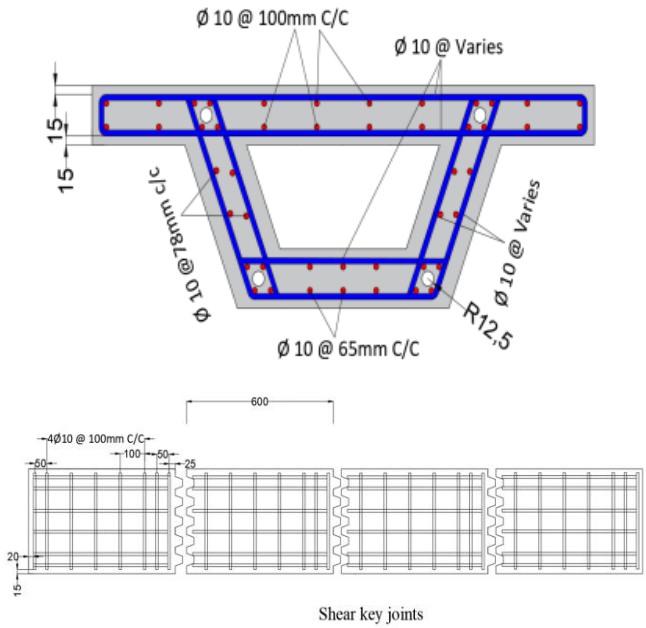

Fig. 3 Reinforcement details and location of the post-tension ducts

Fig. 4 Post-tensioning process of segmental beams and applying jacking force of 137 kN

2.3. Material Properties and Mix Design

Concrete mixes were designed to have the desired workability and mechanical properties to flow easily through the reinforcing cages without segregation and/or separation.

2.3.1. The Materials Used

- Ordinary Portland cement was used in this investigation, CEM-I 42.5R MASS CEMENT, produced in Kurdistan/Iraq.
- The type of silica fume used was MICRO SILICA SUPAFLO – MS90.
- High-performance concrete superplasticizer (Supaflo PC200) to obtain a workable concrete having a low water/binder ratio under ASTM C494-Type A & G.
- Crushed natural coarse aggregate with a maximum aggregate size of 12.5 mm.
- River sand under ASTM C33 [7] specifications.
- Ordinary drinking water was used to mix and cure all kinds of concrete.

2.3.2. Mix Design

For 78.6 MPa, mixing of materials was done in a rotary mixer having a capacity of 0.1 m3; the materials (gravel & sand) were dry mixed for 3-5 minutes. Then the mixture of pre-mixed Silica Fume and cement was added to the aggregates, and the mixer started to mix for additional 3 – 5 minutes. After that, the pre-mixed water with superplasticizer was added gradually with continuous mixing for about three more minutes to react with the binders. The same procedure was applied for the 43.3 MPa mix except for the addition of silica fume and superplasticizer. Table 2 illustrates the details of the designed mix proportions.

2.4. Fabrication of the Test Specimens

For the joint faces of all segments, steel molds using an AutoCAD-controlled cutting machine with a very precise geometry were fabricated and used. Reinforcement cages were accurately assembled inside the molds Fig. 5, and casting was done accordingly. According to AASHTO-2017 requirements, an epoxy layer of 1-2 mm was applied to the joint faces, and female keys were filled with epoxy prior to post-tensioning. The post-tensioning process initially applied 15% of jacking force to each strand and then to full tension immediately. The excess epoxy was squeezed out at full force, and a uniform closure at joints was achieved.

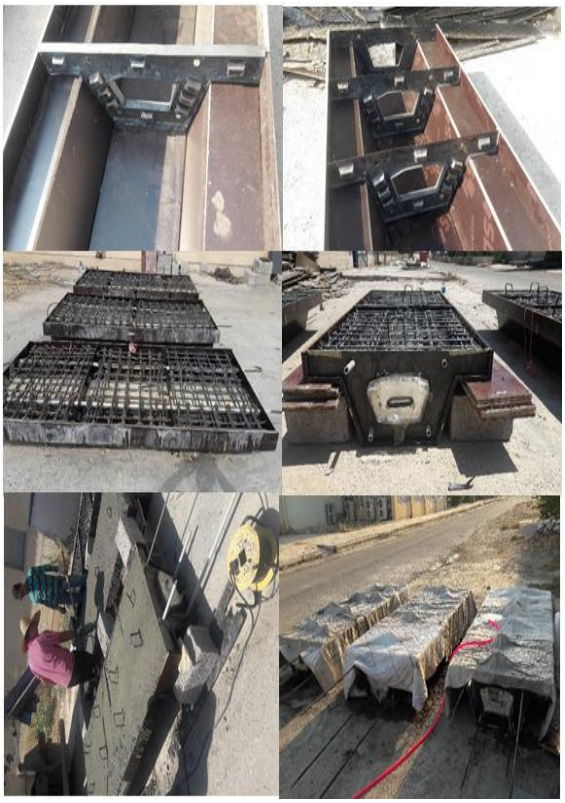

Fig. 5 Fabrication and curing of the test specimens

Table 1 Details of the segmental beams

Specimen No:	Specimen ID	Compressive strength (MPa)	Number of segments	Length of segments (mm)	Span / Depth ratio	No. of shear keys	Type of Joint
1	G1-40-2	43.3	2	1200	3.2	10	Epoxide
2	G1-40-3	43.3	3	800	2.13	20	Epoxide
3	G1-40-4	43.3	4	600	1.6	30	Epoxide
4	G3-80-2	78.6	2	1200	3.2	10	Epoxide
5	G3-80-3	78.6	3	800	2.13	20	Epoxide
6	G3-80-4	78.6	4	600	1.6	30	Epoxide

Table 2 Mix design proportions

Mix No.	Mix proportion C : S : G by weight	Water/Cement ratio	Silica fume %	Admixture / cement %	Target compressive strength (MPa)	Achieved compressive strength (MPa)
1	1:1.33:2.67	0.42	-	-	40	43.3
2	1:1.5:2.36	0.28	14	1.2	80	78.6

2.5. Test Setup and Instrumentation

2.5.1. Test Setup

The tests were carried out in the concrete laboratory in the civil engineering department of Salahaddin University in Erbil. The testing machine has a capacity of 2500 kN consists of a steel frame, as shown in Fig. 6. The loads were applied on the beams through a hydraulic circular jack to a 150mm x 100mm steel beam, two 70 mm plates were used to transfer the vertical loads as two-point loads to the specimens. The distance between the point loads was 0.5 m to obtain pure bending flexural failure.

Fig. 6 Testing machine with the capacity of 2500 kN

2.5.2. Instrumentation

During each test, several measurements were recorded, including applied load, first crack location, ultimate load, and a mechanical dial gauge having an accuracy of 0.01 mm to obtain the deflection of the vertical beam at mid-span, as illustrated in Fig. 7. Beams with compressive strength of 43.3 MPa were loaded at the age of 28 days, and the beams with 78.6 MPa - at 56 days.

Fig. 7 Dial gauge located at mid-span

2.5.3. Loading Test

The loading was carefully and slowly applied at small increments of roughly 5 kN. The values of deflections at mid-span and concrete strains were recorded until failure, at which the ultimate load was recorded.

3. Test Results and Discussion

All specimens' cracking and failure loads and other parameters are shown in Table 3 and the failure patterns for all specimens of groups 1 & 2 - in Fig. 11 and 12.

3.1. Effect of Concrete Compressive Strength (f'c)

When the effect of fc' is considered from the results obtained from the test in Table 3, it is obvious that the specimens with higher f'c from group 2 provided more resistance prior to the appearance of the first crack and failure loads in comparison to the specimens from group1 with lower f'c having the same prestressing post-tension loading. Comparing specimen 4 from group 2 and specimens 1 from group 1 and as shown in Fig. 8, both having two segments, the failure load of specimen 4 was greater by 17%. For specimen 5 from group 2 and specimen 2 in group 1, as shown in Fig. 9, with both having three segments, the failure load of specimen 5 was greater by 15%. Finally, from Fig. 10

comparing specimen 6 from group 2 with specimens 3 from group 1 with both consisting of 4 segments, the failure load of specimen 6 came out to be greater by 11.2%.

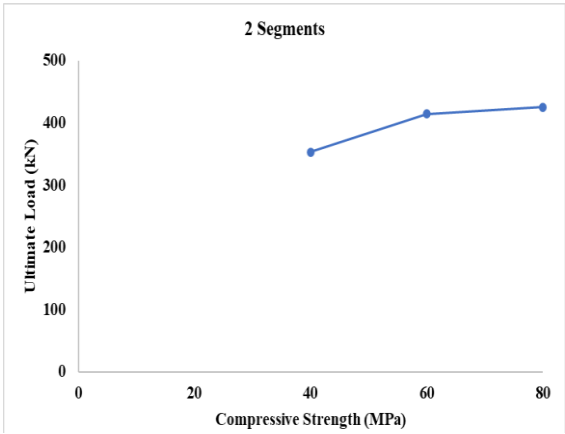

Fig. 8 Curve of ultimate load vs. f 'c for specimens 1 & 4

Table 3 Results obtained from the test for all six specimens

Specimen No.	Specimen ID	F 'c (MPa)	First Crack Load (kN)	Failure Load (kN)	Pcr / Pu %	Deflection at Mid-Span (mm)
1	G1-40-2	43.3	200	353	56.65	21.93
2	G1-40-3	43.3	271	395	68.6	24.42
3	G1-40-4	43.3	215	350	61.4	21.20
4	G2-80-2	78.6	265	425	62.35	23.47
5	G2-80-3	78.6	307	464	66.16	24.90
6	G2-80-4	78.6	240	430	55.82	21.54

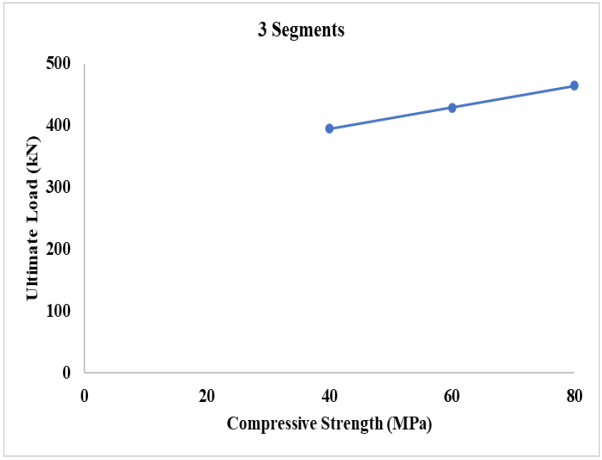

Fig. 9 Curve of ultimate load vs. f 'c for specimens 2 & 5

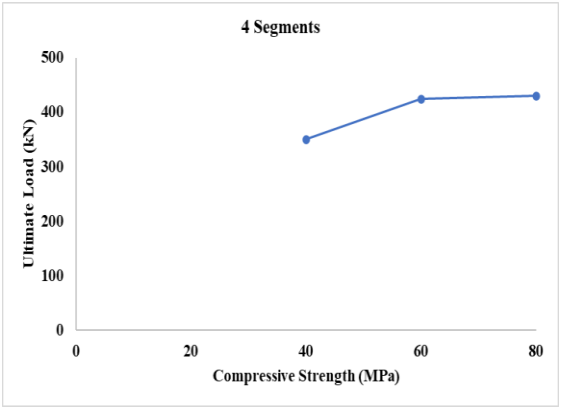

Fig. 10 Curve of Ultimate load vs. f 'c for specimens 3 & 6

3.2. Span to Depth Ratio of Segments (L/D)

Three different segment lengths with a constant total length of the specimens have been tested in this study. In group 1, specimens 1, 2, and 3 consist of 2, 3, and 4 segments having a span/depth ratio of 3.2, 2.13, and 1.6 respectively, and in group 2, specimens 4, 5, and 6 consist of 2, 3 and 4 segments having a span/depth ratio of 3.2, 2.13 and 1.6, respectively. From Table 3, it can be noted that specimen 2 from group 1 consisting of three segments with L/D = 2.13 has a greater ultimate load than specimens 1 having L/D = 3.2 by 10.6%. Also, in group 2, specimen 5, consisting of three segments with L/D = 2.13, has greater ultimate load than specimens 4 by 3.5%. Furthermore, specimens with two segments displayed better resistance than specimens with four segments in both groups. The first crack in the beams with two and four segments in both groups initiated and concentrated close to the face of mid-joint then propagated and spread to the adjacent segment as the applying load increased in which ultimately led to the flexural failure. The beams with three segments in both groups behaved in a different manner because there was no joint at mid-span. When reinforcements continued, the first crack initiated in the near face of both joints propagating along with webs to the mid-span top slab of the beams as shown in Figs. 11 & 12. No cracks were observed in the end segments and anchorage zones.

Fig. 11 Failure crack patterns of specimens 1, 2, and 3 for group 1 (Bending failure)

Fig. 12 Failure crack patterns of specimens 4, 5, and 6 for group 2 (Bending failure)

Figs. 13 & 14 show the relationship of the ultimate load vs. the number of segments in groups 1 & 2. It can be seen that the specimens with three segments achieved a higher ultimate load compared to specimens made from two and four segments.

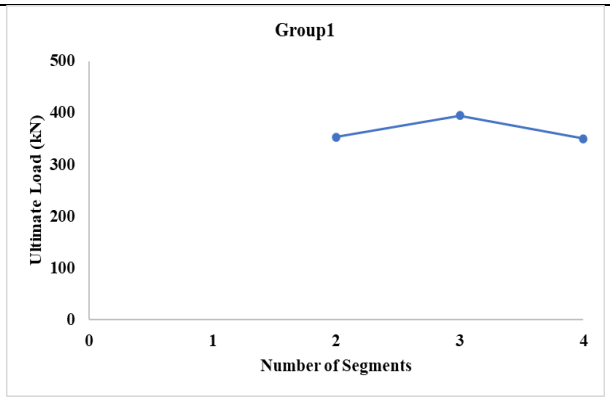

Fig. 13 Ultimate load vs. number of segments relationship for specimens 1, 2 & 3

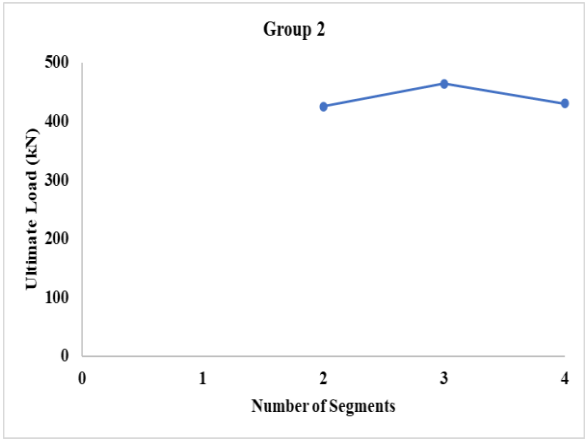

Fig. 14 Ultimate load vs. number of segments relationship for specimens 1, 2 & 3

3.3. Load vs. Deflection

In determining the analysis of the load-deflection relations, two stages in the load-carrying capacity are considered. The first stage was a linear stage that started when the flexural stress intensity was increased; a linear response was observed in vertical deflection for all the specimens. The second stage began directly after the first crack occurrence observed close to the face of the joints for all specimens. The maximum deflection and failure load for all specimens are presented in Table 3. The load-deflection curves for groups 1 and 2 separately and combined are shown in Figs. 15, 16, and 17.

Fig. 15 shows the load-deflection curves for the specimens of group 1. Specimen 2, consisting of three segments, shows the considerably greater flexural capacity and more deflection than specimens 1, 3 because of the continuity of the reinforcements at the mid-span of the beam, which ultimately improved the ductility of the segmental beam. Specimens 1, 3 provided similar bearing capacity and deflection due to segment joint at the mid-span of the girder and discontinuity of the reinforcements in the mid-span of the segments.

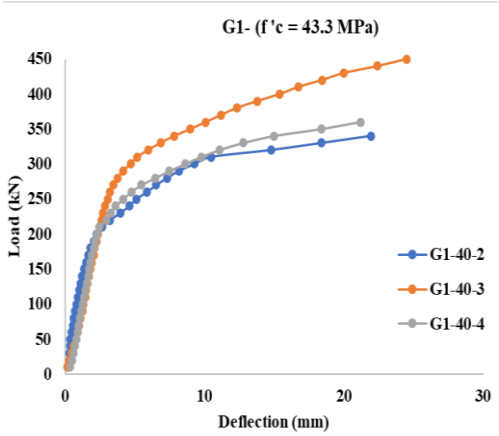

Fig. 15 Load vs. deflection relationship for group 1, specimens 1, 2 and 3

While the load-deflection curves for group 2 specimens are shown in Fig. 16, the beam with three segments (specimen 5) demonstrated greater flexural capacity and more deflection than specimens 4, 6, most likely for the same reason mentioned. In general, group 2 specimens showed better bearing capacity than those of group1 specimens because of having a greater compressive strength of concrete. Finally, the load-deflection curves for all the specimens have been compared and shown in Fig. 17.

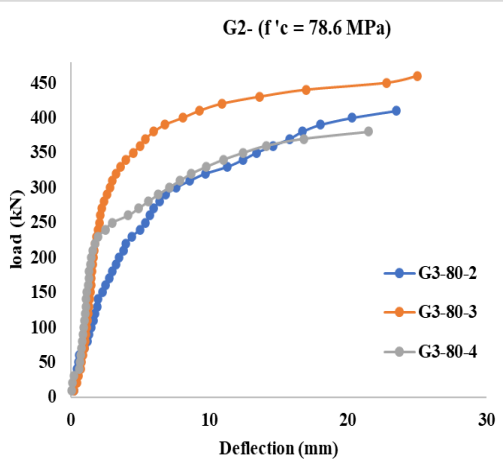

Fig. 16 Load vs. deflection relationship for group 2, specimens 4, 5 and 6

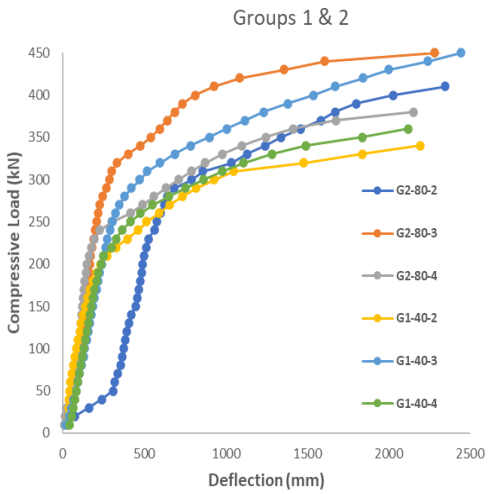

Fig. 17 Load vs. deflection relationship for all specimens

3.4. Load vs. Strain

The positive strain values represent a tensile strain on the bottom surface of the concrete. Some of the strain gauges on the bottom surface of concrete might have been at locations where concrete cracks formed. Therefore, the results of these strain gauges were stopped before reaching the ultimate capacities of the beams. In contrast, the negative strain values indicate a compressive strain on the top surface of the concrete. Each curve of strains on the top surface involves three regions with two turning points. The first turning point designates the initial cracks in concrete. The second turning point indicates yielding in the steel reinforcement or the post-tensioned tendons.

The relationship between vertical applied load and the strains at mid-span bottom slab in the longitudinal direction for all g specimens is shown in Fig. 18. The tensile strains at the bottom slab of the specimens were not like that expected for non-prestressed girders, and they recorded relatively small strain values. The tensile stresses at the bottom of the segmental girders shall initially overcome the compressive force on the bottom of the girders and then begin to produce tensile stresses. At ultimate load, the concrete strain of specimen 4 was more than all specimens. The maximum strain recorded at the bottom slab was 1576 μs for specimen 4, and the minimum strain recorded was 560 μs by specimen 2. It can be noticed that all specimens show similar behavior at the linear stage and then different behavior beyond this stage. Specimens 4 & 6 seem to have a midway shift, which indicates a generation of non-visible cracks at the bottom of the girders.

Fig. 19 shows the relationship between the load and the strains at the mid-span top slab of all the specimens. Specimen 4 recorded the highest strain of 1834 μs at ultimate load, while minimum strain was recorded by specimen 1.

Load versus strain relationship at near supports for all specimens are shown in Fig. 20. The maximum strain is recorded by specimen 6, while specimen 2 recorded minimum at ultimate load. Finally, the load versus strain of all specimens at steel reinforcement is shown in Fig. 21. Specimens 7 and 5 recorded maximum and minimum strains, respectively.

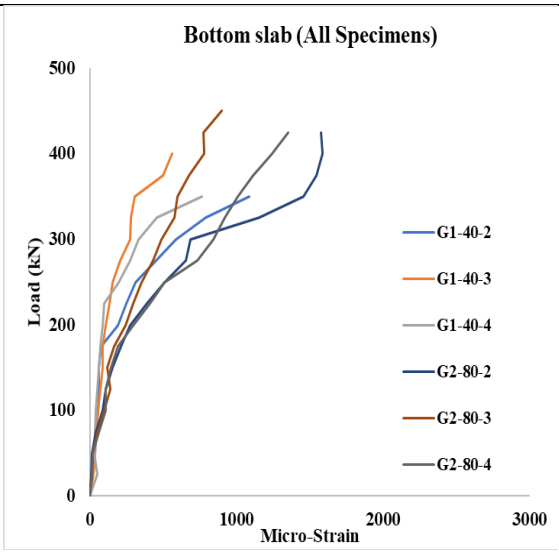

Fig. 18 Load-strain relationship for concrete at mid-span bottom slab for all specimens

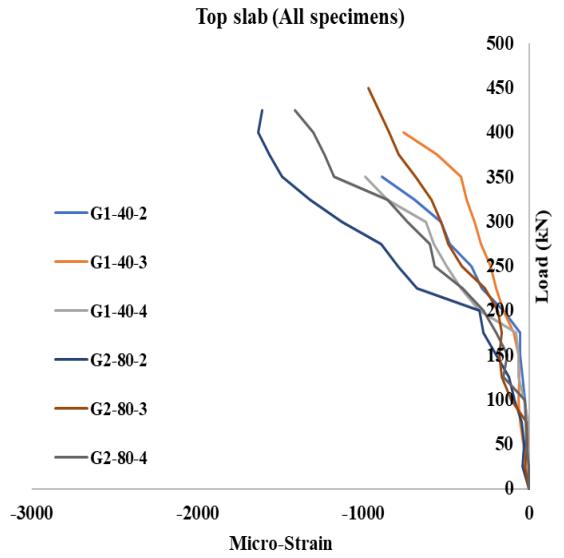

Fig. 19 Load-strain relationship for concrete at mid-span top slab for all specimens

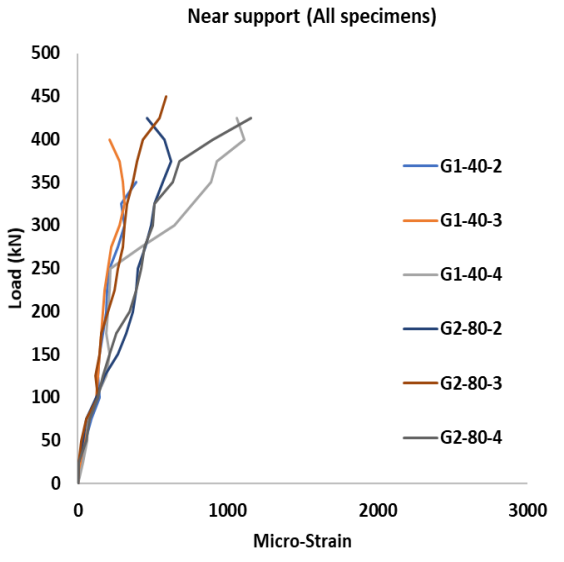

Fig. 20 Load-strain relationship for concrete at near supports for all specimens

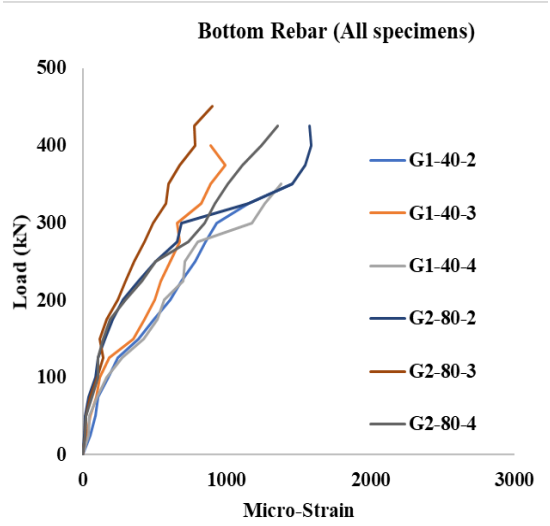

Fig. 21 Load-strain relationship for steel reinforcements at mid-span bottom slab for all specimens

4. Conclusion

Various research and investigations have been performed on the flexural behavior of box girder bridges in general. However, very little attention has been paid to the effect of segment length at different compressive strengths of concrete on such bridges. When segmental box girder bridges are studied, it is essential to understand the span to depth ratio (L/D) of the segments used as they directly influence the flexural performance of such bridges.

This work studied the flexural behavior of precast post-tensioned concrete segmental box girder under flexural loading. The following conclusions have been drawn:

- The compressive strength of concrete (f ‘c) had a significant influence on the flexural behavior in such a way that the specimens in group 2 having fc’ of (78.6 MPa) had a greater response up to 15% to the ultimate load compared with specimens in group1 with fc’ of (43.3).

- Specimens 2 & 5, consisting of three segments, recorded greater ultimate loading than the specimens with two and four segments.

- The specimens 2 and 5, both having three segments, had larger deflections at mid-span compared to the specimens with two and four segments because of their capability to resist more flexural loading.

- The first visible cracks occurred at load levels of 56.65-61.4% and 55.82-66.16 of ultimate loads for groups 1 & 2.

Though quite good results have been observed, it is essential to study more about the flexural behavior by introducing various parameters such as using different post-tensioning systems, increasing the number of strands, using even higher compressive strength of concrete, and increasing the number of shear keys to

drawing strong conclusions. This study is an ongoing project; further work is currently underway.

Acknowledgment

The authors acknowledge the cooperation and support provided by the Concrete and Structures Lab of Salahaddin University / College of Engineering.

References

[1] AMERICAN SEGMENTAL BRIDGE INSTITUTE. *AASHTO-PCI-ASBI Segmental Box Girder Standards for Span-by-Span and Balanced Cantilever Construction*. ASBI, Austin, TX, USA, 2003.

[2] AHMED G.H., and AZIZ O.Q. Influence of intensity and eccentricity of post-tensioning force and concrete strength on shear behavior of epoxied joints in segmental box girder bridges. *Construction and Building Materials*, 2019, 197: 117-129, https://doi.org/10.1016/j.conbuildmat.2018.11.220

[3] AHMED G. H., and AZIZ O. Q. Shear behavior of dry and epoxied joints in precast concrete segmental box girder bridges under direct shear loading. *Engineering Structures*, 2019, 182: 89-100. https://doi.org/10.1016/j.engstruct.2018.12.070

[4] Al-SHERRAWI M.H., ALLAWI A.A., Al-BAYATI B.H., AL GHARAWI M., and EL-ZOHAIRY A. (2018) Behavior of Precast Prestressed Concrete Segmental Beams. *Civil Engineering Journal*, 2018, 4(3). http://dx.doi.org/10.28991/cej-0309109

[5] ASTM. *ASTM A615 Standard Specification for Deformed and Plain Carbon-Steel Bars for Concrete Reinforcement*. ASTM International, West Conshohocken, PA, 2016.

[6] ASTM. *ASTM A416 Standard specification for steel strand, uncoated seven-wire for prestressed concrete*. ASTM International, West Conshohocken, PA, 2018.

[7] ASTM. *ASTM C33 Standard specification for concrete aggregates*. ASTM International, West Conshohocken, PA, 2018.

[8] CHAI S., GUO T., CHEN Z., and YANG J. Flexural Behavior of Precast Concrete Segmental Box-Girders with Dry Joints. *Advances in Civil Engineering*, 2020, Article ID 8895180. https://doi.org/10.1155/2020/8895180

[9] HUANG D., and HU B. Evaluation of Cracks of Hathaway Precast Concrete Segmental Box Girder Bridge. In: *18th IABSE Congress: Innovative Infrastructures – Towards Human Urbanism, Seoul, Korea, 19-21 September 2012*, published in *Innovative Infrastructures – Towards Human Urbanism*, 2012: 1758-1765. https://doi.org/10.2749/222137912805112554.

[10] TITO J.A., and GOMEZ-RIVAS A. Design, Construction, and Test of a Posttensioned Segmental Beam. In: *Ninth LACCEI Latin American and Caribbean Conference, Engineering for a Smart Planet, Innovation, Information Technology and Computational Tools for Sustainable Development, August 3-5, 2011, Medellín, Colombia*, 2011.

[11] WRAYOSH W.A., and HASHIM A.H. Flexural Behavior of Box Segmental Beams with Internal Tendons Subjected to Repeated and Static Loads. *IOP Conference Series: Materials Science and Engineering*, 2020, 671.

[12] YUAN A., HE Y., DAI H., and CHENG L. Experimental Study of Precast Segmental Bridge Box Beams with External Unbonded and Internal Bonded Posttensioning under Monotonic Vertical Loading. *Journal of Bridge Engineering*, 2015, 20(4): 04014075. https://ascelibrary.org/doi/10.1061/%28ASCE%29BE.1943-5592.0000663.

[13] YUAN A., WU W., SUN D., and DAI H. Experimental on Flexural Behavior of Segmental Precast Concrete Beam with Internal Tendons and External Tendons. *Journal of Chang'an University: Natural Science Edition*, 2015, 35(5): 73-81.

參考文:

[1] 美國分段橋樑學院。美國國家公路和運輸官員協會-預應力混凝土協會-美國分段橋樑學院跨跨和平衡懸臂結構的節段箱樑標準。美國分段橋樑學院，美國德克薩斯州奧斯汀，2003 年。

[2] AHMED G.H. 和 AZIZ O.Q.後張力強度、偏心距和混凝土強度對節段箱樑橋環氧樹脂節點抗剪性能的影響.建築與建材, 2019, 197, 117-129, https://doi.org/10.1016/j.conbuildmat.2018.11.220

[3] AHMED G. H. 和 AZIZ O. Q. 在直接剪切載荷下預製混凝土節段箱樑橋中乾式和環氧樹脂接頭的剪切行為。工程結構，2019，182：89-100。https://doi.org/10.1016/j.engstruct.2018.12.070

[4] Al-SHERRAWI M.H.、ALLAWI A.A.、Al-BAYATI B.H.、AL GHARAWI M. 和 EL-ZOHAIRY A. (2018) 預製預應力混凝土分段樑的行為。土木工程雜誌, 2018, 4(3). http://dx.doi.org/10.28991/cej-0309109

[5] 美國材料試驗學會。 美國材料試驗學會 A615 用於混凝土鋼筋的變形和普通碳鋼棒的標準規範。 美國材料試驗學會 國際，賓夕法尼亞州西康斯霍肯，2016 年。

[6] 美國材料試驗學會。 美國材料試驗學會 A416 預應力混凝土用無塗層七線鋼絞線標準規範。 美國材料試驗學會 國際，賓夕法尼亞州西康斯霍肯，2018 年。

[7] 美國材料試驗學會。 美國材料試驗學會 C33 混凝土骨料標準規範。 美國材料試驗學會 國際，賓夕法尼亞州西康斯霍肯，2018 年。

[8] CHAI S., GUO T., CHEN Z. 和 YANG J. 帶乾接縫的預製混凝土節段箱樑的彎曲行為。土木工程進展，2020 年，文章身份證明文件8895180。https://doi.org/10.1155/2020/8895180

[9] HUANG D. 和 HU B. 海瑟威預製混凝土節段箱樑橋裂縫評價。在：第 18 屆國際橋樑與結構工程協會大會：創新基礎設施——邁向人類城市主義，韓國首爾，2012 年 9 月 19-21 日，發表在創新基礎設施——邁向人類城市主義，2012：1758-1765。https://doi.org/10.2749/222137912805112554。

[10] TITO J.A. 和 GOMEZ-RIVAS A. 後張式分段樑的設計、施工和測試。在：第九屆拉丁美洲和加勒比工程機構聯盟拉丁美洲和加勒比會議，智能地球工程、創新、信息技術和可持續發展計算工具，2011 年 8 月 3 日至 5 日，哥倫比亞麥德林，2011 年。

[11] WRAYOSH, W.A. 和 HASHIM, A.H. 內部肌腱承受重複和靜態載荷的箱形分段樑的彎曲行為。物理研究所會議系列：材料科學與工程，2020，671。

[12] YUAN A., HE Y., DAI H. 和 CHENG L. 單調垂直荷載下外無粘結和內粘結後張法預製分段橋箱樑的試驗研究。橋樑工程學報, 2015, 20(4): 04014075. https://ascelibrary.org/doi/10.1061/%28ASCE%29BE.1943-5592.0000663。
[13] YUAN A., WU W., SUN D. 和 DAI H. 帶內筋和外筋節段預製混凝土樑的彎曲性能試驗。長安大學學報: 自然科學版, 2015, 35(5): 73-81.